SUBSURFACE HYDROLOGY

Vadose zone infiltration rate at Hanford, Washington, inferred from Sr isotope measurements

Katharine Maher[†, §], Donald J. DePaolo[†, §], Mark E. Conrad [§], R. Jeff Serne[*]

[†] *Earth Sciences Division, E.O. Lawrence Berkeley National Laboratory, Berkeley, California*

[§] *Department of Earth and Planetary Science, University of California, Berkeley*

[*] *Pacific Northwest National Laboratories, Richland, Washington.*

ABSTRACT

Sr isotope ratios were measured in the pore water, acid extracts, and sediments of a 70-meter vadose zone core to obtain estimates of the long-term infiltration flux for a site in the Hanford/DOE complex in eastern Washington State. The $^{87}Sr/^{86}Sr$ values for the porewaters decrease systematically with depth, from a high value of 0.721 near the surface towards the bulk sediment average value of 0.711. Estimates of the bulk weathering rate combined with Sr isotopic data were used to constrain the infiltration flux for the site given both steady state and non-steady state conditions. The models suggest that the infiltration flux for the site is 7 to 12 mm/yr. The method shows potential for providing long-term *in situ* estimates of infiltration rates for deep heterogeneous vadose zones. (Index Terms: 1040 (Isotopic composition/chemistry), 1875 (Unsaturated Zone), 1045 (Low-temperature Geochemistry), 1886 (Weathering, (1625)) and 3210 (Modeling)).

1. INTRODUCTION

The rate of recharge from meteoric sources to the water table is a critical input parameter for groundwater models in arid regions. Several methods for estimating recharge are commonly employed, including chloride mass balance, soil lysimeter studies, and tensiometer/soil water balance methods [*Murphy et al.*, 1996; *Campbell et al.*, 1991; *Rockhold et al.*, 1990; *Routson and Johnson*, 1990]. These methods provide useful results in many circumstances, however, infiltration rates are inherently difficult to quantify in regions where recharge is small. Considering the importance of infiltration in arid regions, additional approaches would be useful if they can be proven accurate. In this paper we present the results of Sr isotope measurements of vadose zone materials from the semi-arid central plateau region of the Hanford Reservation in south central Washington. We interpret the Sr isotopic data as a measure of the long-term infiltration flux, given certain assumptions and approximations. The derived infiltration fluxes are in qualitative agreement with the results of other approaches.

Infiltration rates at the Hanford/DOE site in Washington are of particular concern because substantial quantities of radioactive waste material have been disposed into the surface soils and vadose zone sediments with the expectation that ion exchange processes would retain most of the radionuclides in the vadose zone and prevent them from reaching groundwater [*USDOE*, 1987]. While these expectations were met in many cases, the large inventory of radionuclides resident in the subsurface, coupled with the regulatory need to specify probable groundwater contamination levels hundreds or thousands of years into the future, requires that migration of radionuclides through the

vadose zone be accurately assessed [*Hartman*, 1998]. In addition, modifications to the surface character of the site, damage to containment structures, water-line leaks, and industrial water disposal on the surface, have resulted in significant increases in infiltration rates and recharge in many areas [*Gee et al*., 1992]. Accurate estimates of infiltration rates, for both the present and long-term forecasts, are critical to predicting radionuclide migration and assessing remediation options. Recharge is also important for understanding groundwater chemistry and the potential for contaminated discharge to the Columbia River [*Fayer et al.,* 1995].

Using chloride mass balance and soil lysimeter studies, recharge values ranging from <0.01 mm/yr [*Campbell et al.,* 1991*; Murphy,* 1996] to 200 mm/yr [*Rockhold et al.,* 1990] have been proposed for various study sites around the Hanford Area. These values compare to an average annual rainfall of 162 mm/year [*Gee et al.,* 1992]. The infiltration flux values determined have been dependent on vegetation and the coarseness of the surface soils—fine-grained vegetated soils yield the lowest values and bare gravelly soils yield the highest recharge rates [*Gee et al.*, 1992; *Campbell et al.*, 1991; *Rockhold et al*., 1990]. Where it has been possible to compare methods, agreement has not always been acceptable [*Gee et al,* 1992]. The most reliable estimates are those made at monitoring sites where infiltration has been measured directly (e.g. the 200-East Closed-Bottom Lysimeter [*Routson and Johnson*; 1990 and *Rockhold et al.*, 1990] and the 300-Area Buried Waste Test Facility (BWTF) [*Rockhold et al.*, 1990]). Most of these monitored sites are near waste disposal areas where the hydrological characteristics have been recently disturbed resulting in higher infiltration fluxes [*Gee et al.,* 1992]. There

are still few measurements available for the site overall, and estimates representative of long-term average fluxes (hundreds to thousands of years) are fewer still.

Strontium isotope measurements of vadose zone pore fluids and soil matrices can in theory provide *in situ* long-term estimates of infiltration flux. The use of Sr isotope measurements to provide information regarding water-rock interaction and the movement of groundwater in both saturated and unsaturated porous media is described in detail by *Johnson and DePaolo* [1994, 1997*a,b*], *Bullen et al.* [1996] and *Johnson et al.* [2000]. The method is being used to provide constraints on both modern and ancient vadose zone infiltration at Yucca Mountain [*Sonnenthal and Bodvarsson,* 1999]. Strontium isotopes have also been used in the study of pore fluids in the deep-sea environment [*Baker et al*., 1989; *Richter and DePaolo*, 1988; *Richter*, 1993]. Groundwater entering a specific rock or soil environment typically contains dissolved Sr in low concentration (ca. 100 μg/L total Sr) with an isotopic ratio ($^{87}Sr/^{86}Sr$) that is in general different from mineral phases in soil matrices that are undergoing weathering. Weathering results in the dissolution of primary minerals and introduces Sr to the pore fluid with an $^{87}Sr/^{86}Sr$ ratio that is the same as the weathering minerals. Weathering processes shift the $^{87}Sr/^{86}Sr$ of the porewater Sr toward that of the dissolving minerals. Removal of dissolved Sr by secondary mineral precipitation and ion exchange prevents the total pore fluid Sr concentration from being a direct reflection of mineral dissolution [*Johnson and DePaolo*, 1994]. However, the $^{87}Sr/^{86}Sr$ ratio of the pore fluid does respond in a linear fashion to mineral dissolution. In groundwater moving through a soil matrix, the rate of change of the pore fluid $^{87}Sr/^{86}Sr$ value is a measure of the ratio of the fluid Sr flux to the local soil dissolution Sr flux. Given that the Sr concentrations and isotopic ratios can be

measured in both the fluid phase and the dissolving mineral phases, the change in $^{87}Sr/^{86}Sr$ with depth in the fluid phase can be used to derive a value for the ratio of the weathering rate (R_d) to the fluid flux. Estimates of weathering rates can then be used to calculate values for the fluid flux.

An important characteristic of the Sr isotope method is that the derived estimate of infiltration rate is likely to be an average value representing hundreds to thousands of years. This information is useful in light of the need for predictions that extend at least that far into the future. Recent disturbances to the hydrology of the site are also unlikely to affect the results, since the exchangeable pool of Sr in the soils is commonly large enough to preserve a memory of the pre-industrial conditions [*Johnson and DePaolo,* 1997*a,b*]. The method does not require introduction of tracers, or disturbance of the site hydrology beyond the drilling required for obtaining subsurface samples. Because the Sr isotope method uses different assumptions than the chloride mass balance approach, the two methods should be complementary.

2. SAMPLING AND ANALYTICAL TECHNIQUE

2.1 Hydrogeologic Setting

The Hanford/DOE Site in central Washington is situated within a broad plain formed by Miocene-age tholeiitic basalt flows of the Columbia River Basalt Group. The site lies within the Pasco Basin, one of the larger sub-basins of the Columbia Plateau, and is bounded on the west by a basaltic ridge, Rattlesnake Mountain, and on the north and east by the Columbia River (Figure 1). The basalt flows in this region are overlain by

Pliocene- to Pleistocene-Age sedimentary deposits. The lithostratigraphic units are shown in Figure 2.

Surface soils in the 200 Area plateau consist of coarse-textured Holocene alluvial sands mantled by fine-grained eolian sheet sands [*Lindsey*, 1994]. Beneath the surface layers are the cataclysmic flood and inter-flood deposits that compose the Pleistocene Hanford Formation (Figure 2). In the 200 West Area, the heterogeneous Hanford Formation is divided into several sub-facies: a medium-grained sand (HFSD1), a pebble gravel (HFGD), and another fine to coarse-grained sand and interbedded silt unit (HFSD2) [*US DOE*, 2002]. The cataclysmic Pleistocene flooding that deposited the Hanford Formation ended approximately 13,000 years ago [*Mann et al.*, 1997]. Underneath the Hanford Formation is the Pliocene Cold Creek Unit (CCUf(lam-mas), a facies composed of intercalated layers of fine sand and silt and some weakly developed paleosols [*US DOE*, 2002]. The upper Cold Creek Unit blankets a coarse to fine-grained, $CaCO_3$ cemented facies (CCUc-f(calc) which developed unconformably on top of the Ringold Formation. This lower unit is representative of a weathered paleosurface and is approximately 40 wt% $CaCO_3$ in the 299-W22-48 borehole [*Serne et al.*, 2002a,b].

Average annual precipitation at the Hanford site over the past 80 years is 162 mm/yr. Precipitation falls mainly during the winter months when humidity is relatively high and evaporation low [*Gee et al.*, 1992]. Rapid snowmelt events, intense thunderstorms and periodic droughts cause precipitation and infiltration to vary both regionally and temporally. The depth to the water table at the study site is approximately 70 meters (Figure 1b and 2). Groundwater flow in the upper unconfined aquifer at the borehole location is predominantly from northwest to southeast. The majority of the

focused regional recharge occurs in the vicinity of areas where the Columbia River Basalt is exposed at the surface, to the west and south of the 200 Area (Figure 1b). Large volumes of water were disposed in surface ponds to the west of the study site (mainly at U Pond), creating local transient mounds of steep, radial hydraulic gradients [*Hartman*, 1998].

The vegetation at the site consists of shrub-steppe plant communities composed of annual and perennial grasses and shrubs of mixed rooting-depths. Perennial shrubs, including sagebrush (*Artemesia tridentata* Nutt.) and rabbitbrush (*Chrysothamnus nauseosus* Pallus) that have deep rooting structures can have a dramatic effect on the recharge in coarse-textured soils [*Rockhold et al.*, 1990]. Most of the vegetation within the waste burial grounds and tank farms has been removed due to concerns over the intrusion of deep plant roots into the waste sites. The removal of vegetation, which occurred within the past 50 years, may have increased the infiltration rates [*Gee et al.*, 1992].

2.2 Sample collection and preparation

The isotopic compositions (Sr, $\delta^{18}O$, and D) of pore water samples and bulk sediment were analyzed for a 72-meter borehole adjacent to one of the waste storage areas in the 200 Area plateau (Figure 2). The core is presumed to be in an area uninfluenced by site activities beneath a depth of approximately 2-3 meters. The core samples were obtained during the installation of a monitoring well in October of 1999. Gravimetric water content measurements on an oven-dry basis were taken at Pacific Northwest National Laboratory, for both split-spoon sleeves and core samples. The water content and chemical data of Figure 3 are reported in *Serne et al.* [2002b]. Separate core

samples were obtained by Lawrence Berkeley National Laboratory (LBNL) for the Sr isotope, total Sr concentrations, and stable isotope measurements. For determination of stable isotope values and water content, the soil water was extracted by heating the sediment for variable time at 100°C under a vacuum extraction line at LBNL. This procedure was assumed to exclude the dissolved constituents, which were later captured in the pore water rinses. The moisture content for LBNL samples was determined by weighing the sediment before and after the pore water extraction and is tabulated in Table 2. The LNBL and PNNL gravimetric water contents are generally in very good agreement. Following the vacuum extraction procedure, pore water rinses and warm nitric acid leaches were performed using 150 g of homogenized dry sediments. For the pore water rinses, 30 g of sediment were combined with 30 ml of 18MΩ de-ionized water, shaken for 90 minutes and allowed to stand for 24 hours. The strontium contained in the rinse water is assumed to be that which was originally dissolved in the pore fluid, plus any readily exchangeable strontium on the solid phases. For the nitric acid leaches, 5 g of soil were combined with 15 ml of double-distilled 8N nitric acid and heated for 6-8 hours at 70°C then allowed to cool over night. After 24 hours, the leach solutions were vacuum filtered through a 0.45 μm polyethylene filter into screw-top polyethylene bottles. Bulk sediment Sr concentrations were measured at LBNL for 300 mg splits dissolved in a mixture of concentrated perchloric and hydrofluoric acids. The mixture was evaporated to dryness and re-dissolved in 3N nitric acid prior to the chemical separations. Bulk sediment Sr concentrations were also measured by XRF methods at PNNL [*Serne et al.*, 2002a,b]. Mineral separates for the sediments were obtained by

magnetic separation and handpicking, and were analyzed for $^{87}Sr/^{86}Sr$, $^{87}Rb/^{86}Sr$ and K, Rb and Sr concentrations following the same dissolution procedure as above.

All Sr samples (water, acid, bulk sediment digestions, and splits from mineral separates) were purified by ion exchange chromatography using Eichrom Sr- Spec resin in 0.250 ml Teflon columns. Yields for the chemical separations are about 98%. Total procedural blanks were approximately 5 and 45 ng Sr for the deionized water and 8N nitric acid leach respectively, corresponding to <0.2%-0.1% of the total amount of Sr extracted. Given the small contribution from blank relative to the total amount of Sr analyzed, no blank corrections were applied.

Sr isotopic ratios were measured on a VG354 multi-collector thermal ionization mass spectrometer. The average value for NBS 987 during the analyses was 0.710286 ± 0.00002 (2σ). Stable isotope measurements are reported in *DePaolo et al*. [2002].

3. RESULTS

The volumetric water content (θ) and corresponding lithology (measured by *Serne et al.* [2002b]) are shown in Figure 2. The gravimetric water contents of *Serne et al* [2002b] and those measured at LBNL (Table 1) were converted to volumetric water content assuming a constant bulk density of 1.9 mg/L. The agreement between the two data sets is satisfactory, however, because of greater sampling resolution we chose to depict the data from *Serne et al.* [2002b] in Figure 2. The average water content of the sediments is 9% by volume, but vaires from 3% to 39%. The water content is notably elevated at 26 to 32 meter depth in the HFSD2 Formation, at 44.5 m in the lower Cold Creek caliche layer, and at 52 meters corresponding to a clastic dike in the Ringold Formation. There is close correlation between the elevated water content and the finer-

grained units, which is most likely due to the capillary barrier phenomenon that allows the water content to increase in fine-grained sediments underlain by coarse grained sediment [*Stormont et al.*, 1999].

The upper HFSD1 facies of the Hanford Formation is composed predominantly of sand (~90%) and inter-bedded silt and clay layers (~8%) with slightly higher water contents (Table 1b). The gravel-dominated HFGD unit is the most coarse in composition, ranging from 63.2% gravel and 36% sand, to 3% gravel and 92% sand at the contact with the finer-grained lower HFSD2 unit (94%-98% sand). The silt and clay contents were highest in the Cold Creek units (38.6%), whereas the Ringold Formation is predominantly sand and silt [*Serne et al.*, 2002b].

The mineralogical composition of the sediments for selected depths is shown in Table 1a. The sediments are predominantly composed of quartz, plagioclase, alkali feldspar, and accessory minerals such as biotite, calcite, and clays. The most notably different layer is the lower Cold Creek unit (CCUc-f(calc), which has a calcite content of 40%. The upper Hanford Formation facies are particularly rich in quartz and depleted in alkali feldspar relative to the lower formations.

Profiles of the chemical data for the pore water rinses are shown in Figures 3a and 3b [*Serne et al.*, 2002b]. The pH values show two prominent spikes, one in the middle of the HFSD unit (~33 m) and another at the base of the caliche layer. These elevated pH values correspond to elevated concentrations of the base cations, Ca, Mg and Na (Figure 3b). Chloride measurements show a bulge at 32 meters that corresponds to the elevated water content in the lower HFSD2 unit. Major base cations are fairly constant with depth,

showing a slight decline throughout the Ringold Formation and a major spike at the lower Cold Creek unit.

The $^{87}Sr/^{86}Sr$ values and total Sr concentrations for the pore water rinses, nitric acid leachates, and bulk sediment are presented in Table 2. The $^{87}Sr/^{86}Sr$ values for the pore water rinses decrease systematically from a peak value of 0.721 at a depth of 3 meters to 0.712 at 57 meters depth (Figure 4b). The trend of decreasing $^{87}Sr/^{86}Sr$ extrapolates to a value close to the local groundwater value of 0.710. A significant spike toward high $^{87}Sr/^{86}Sr$ occurs at 38.4 meters, and smaller spikes are observed at 17 meters and 52 meters. The $^{87}Sr/^{86}Sr$ values of the nitric acid leaches are variable, but consistently lower than the values in the distilled water rinses between the depths of 3 and 50 meters. The nitric acid leach of the sediment from 3 meters depth has an especially high value of $^{87}Sr/^{86}Sr$, which is discussed further below. The Sr in the nitric acid leach is presumed to reflect the total exchangeable Sr plus a large contribution from more soluble mineral phases, whereas the water rinse solution is presumed to represent mainly the dissolved Sr in the pore water. Approximately 10 -15% of the total soil strontium was removed by the strong acid leach, based on a bulk sediment strontium concentration of about 325 ppm.

Strontium concentrations calculated for the pore waters vary from 0.1 mg/L to 4.7 mg/L, with an average value of 1.5 mg/L. The shallowest sample, at 0.3 m depth, has a much higher concentration of about 12.7 mg/L. The nitric acid leach values are mostly between 20 and 40 μg/g soil, with the exception of the caliche layer (CCUc-f(calc)) that has much higher concentrations. The sediments below about 52 meters depth have consistently low Sr in the nitric acid leaches.

The $^{87}Sr/^{86}Sr$ and total Sr concentrations for the bulk sediments are fairly constant ranging from 0.7095 to 0.7115 and 325 ppm respectively, with no evident systematic trend (Table 2). The $^{87}Sr/^{86}Sr$ values of the Hanford sediments contrast strongly with those of the Columbia River Basalts that surround and underlie them, which have $^{87}Sr/^{86}Sr$ values of 0.704 to 0.707 [*Hooper and Hawkesworth*, 1993]. To evaluate the relationship between the bulk sediment, the nitric acid leaches, and the pore waters, we measured mineral separates from several horizons. The $^{87}Sr/^{86}Sr$ values and $^{87}Sr/^{86}Sr$ for the mineral separates are shown in Table 3. The highest $^{87}Sr/^{86}Sr$ ratio for the biotite separates (0.71895) is lower than the highest value of the pore water rinses (0.721), and slightly lower than the value for the nitric acid leach from 3 m depth (0.71914). In comparison, the $^{87}Sr/^{86}Sr$ ratios for the feldspar concentrates are much lower, in the range 0.7047 to 0.7093. As expected, the K-feldspar concentrates have higher $^{87}Sr/^{86}Sr$ values than the plagioclase from the same sediment. The Sr concentrations for the biotite separates were in general much lower than the feldspar values, while the $^{87}Rb/^{86}Sr$ values were considerably higher, consistent with the high $^{87}Sr/^{86}Sr$ values (Table 3) .

4. DISCUSSION

4.1 Mineralogic constraints for the Sr isotopic profile

One of the most significant features of the Sr isotope profile is the high value of $^{87}Sr/^{86}Sr$ at a depth of 3 to 5 meters in both the pore water and nitric acid leaches (Figure 4b). ^{87}Sr results from the β-decay of ^{87}Rb ($t_{1/2}$ = 48.8 by) [*Dickin*, 1995]. Some aluminosilicate minerals such as biotite have a high concentration ratio (Rb/Sr) compared to other granitoid minerals, such as K-feldspar and plagioclase. As a result of this

geochemical pattern, the $^{87}Sr/^{86}Sr$ ratios of the above minerals decrease from biotite to K-feldspar to plagioclase. In addition, biotite is known to weather much more rapidly than feldspars [*Blum and Erel*, 1995; *Taylor et al.*, 2000a,b]. Recent studies have found that rapid preferential weathering of biotite in the first 20-50 kyr of soil formation can generate a high- $^{87}Sr/^{86}Sr$ weathering flux to the pore water [*Blum and Erel*, 1995; *Blum and Erel*, 1997; *Bullen et al.,* 1997, *Taylor et al.,* 2000a].

The peak $^{87}Sr/^{86}Sr$ values in the pore water occur just below the peak value of the nitric acid leach, at 3 and 5 meters respectively. The nitric acid leach data indicate the presence of readily dissolving material with exceptionally high $^{87}Sr/^{86}Sr$ at 3m depth. The steep gradient in $^{87}Sr/^{86}Sr$ between the surface and 3m depth indicates that this high-$^{87}Sr/^{86}Sr$ material is weathering rapidly and serves to quickly increase the $^{87}Sr/^{86}Sr$ ratio in downward migrating water. Such high $^{87}Sr/^{86}Sr$ values could be attributed to a larger proportion of radiogenic biotite, whereby high-$^{87}Sr/^{86}Sr$ biotite, coupled with a more rapid weathering rate, releases a radiogenic component to the pore fluid and nitric acid leaches that is not reflected in the bulk sediment values. Experimental weathering studies have shown that differences in the location of the Rb and Sr within the mineral structure of micas may cause the isotopic ratio of Sr released during weathering to be higher than the bulk mineral ratio by as much as 0.1 [*Taylor et al.,* 2000a]. This effect could explain the difference between the highest biotite concentrate $^{87}Sr/^{86}Sr$ value (0.719) and the highest porewater value (0.721).

The $^{87}Sr/^{86}Sr$ values of the pore water from the uppermost samples (0.4 and 2 meters) are similar to both the nitric acid leach values and the values measured in Columbia River water; the latter vary seasonally and are typically in the range 0.7137 to

0.7144 (unpublished data). The isotopic data for the top 2 meters of the pore water profile most likely result from rainfall, which has a very low Sr concentration. The water receives adsorbed Sr from the sediments and hence acquires the isotopic composition of the weathering minerals, which in turn have an $^{87}Sr/^{86}Sr$ ratio close to the value of the nitric acid leaches.

This high-$^{87}Sr/^{86}Sr$ weathering flux present in the upper 5 meters of the section, regardless of the exact mineralogical source, effectively sets the pore water $^{87}Sr/^{86}Sr$ at a high value by a depth of 5 meters. Further infiltration places this water in contact with sediments whose weathering flux has lower $^{87}Sr/^{86}Sr$. The decrease in the $^{87}Sr/^{86}Sr$ values of the nitric acid leaches with depth is most likely due to some natural variation in the isotopic and mineralogic composition of the sediments as a result of the complex sedimentary history of the site. In the modeling described below, our preferred model incorporates the assumption that the $^{87}Sr/^{86}Sr$ ratios of the nitric acid leaches represent the values associated with the bulk flux of Sr released from the soils as a result of dissolution of the primary mineral phases. The gradual shift of pore water $^{87}Sr/^{86}Sr$ with depth is therefore inferred to be the result of either slow addition or exchange of locally derived Sr to (or with) the downward-percolating fluid.

4.2 Sr Isotope Model equations

The equations governing Sr isotope patterns in groundwater are derived in *Johnson and DePaolo* [1997a]. For an adsorbing solute such as Sr with a negligible vapor phase, the solute transport equation for an unsaturated medium can be written as:

$$\left(1+\frac{\rho_b K_d}{\theta}\right)\frac{\partial C_f}{\partial t}=\frac{\partial}{\partial z}\left(D\frac{\partial C_f}{\partial z}\right)-v\frac{\partial C_f}{\partial z}+\sum_{i=1}^{n}J_i \qquad (1)$$

where D is the vertical hydrodynamic dispersion coefficient and C_f is the solute concentration in the pore fluid. The mean pore water velocity is represented by v and the last term, J_i, is the reaction flux representing dissolution (positive value) and precipitation (negative value). Equation (1) is applicable only if it is assumed that the exchange flux between the adsorbed and dissolved phases is much larger than either the advective Sr flux or the source Sr fluxes. For semi-arid vadose zone transport, where advective velocities are typically small, this assumption is valid. Weathering fluxes are also typically small in comparison to exchange fluxes. The first term on the left hand side represents the retardation factor; ρ_b is the bulk density of the soil, θ is the volumetric water content and K_d is the slope of the instantaneous linear adsorption isotherm for the species. Reformulating (1) in terms of an isotope ratio ($^{87}Sr/^{86}Sr$) and assuming that dispersion is constant over depth yields [cf. *Johnson and DePaolo*, 1997*a*]:

$$\left(1+\frac{\rho_b W_e C_e}{\theta C_f}\right)\frac{\partial r_f}{\partial t}=D\frac{\partial^2 r_f}{\partial z^2}-\left[v-\frac{2}{C_f}\frac{\partial C_f}{\partial z}\right]\frac{\partial r_f}{\partial z}+\sum_{i=1}^{n}\frac{J_{di}}{C_f}\left[r_{di}-r_f\right] \qquad (2)$$

C_f and C_e are the Sr concentrations in the fluid and the exchanging solid phase, and r_f is the isotope ratio of the fluid phase. W_e is the mass of the exchanging phase per unit volume of fluid. The reaction fluxes, J_{di} are a result of dissolution processes only, as

precipitation does not change the Sr isotopic composition of the fluid. Each mineral that is undergoing weathering (dissolution) provides a contribution to this flux:

$$J_{di} = MR_{di}W_{di}C_{di} \tag{3}$$

and each mineral has a particular value of the isotopic ratio (r_{di}). R_{di}, W_{di} and C_{di} are, respectively, the fractional dissolution rate of mineral *i* (time^{-1}), the mass fraction of mineral *i* in the solid phase, and the Sr concentration of mineral *i* (per unit mass of the mineral). M is the local solid/fluid mass ratio:

$$M = \frac{\rho_b(1-\phi)}{\rho_f \theta} \tag{4}$$

where ρ_f is fluid density and ϕ is porosity.

The retardation factor for the isotopic ratio may differ from that for the total Sr concentration, as the isotopic ratio is affected only by the amount of adsorbed exchangeable Sr actually present. Denoting the isotopic retardation factor as K_{ret}:

$$K_{ret} = 1 + \frac{MW_eC_e}{C_f} = 1 + \frac{m_e}{m_f} \tag{5}$$

where m_e is the mass of exchangeable Sr in the solid phase per unit volume of sediment, and m_f is the mass of dissolved Sr per unit volume of sediment.

The other terms in equation (2) can also be simplified. The source term can be written in terms of a bulk weathering rate time constant (R_d), a bulk weathering mineral fraction (W_d), and a bulk isotopic ratio for the weathering mineral fraction (r_d). Also, the term modifying the velocity can be ignored for simplicity because unless the fluid Sr concentration is systematically increasing or decreasing by a substantial amount, this term will not affect the inferred velocity significantly. Hence to a sufficiently good approximation, equation (2) can be rewritten in the simpler form:

$$K_{ret}\frac{\partial r_f}{\partial t} = D\frac{\partial^2 r_f}{\partial z^2} - v\frac{\partial r_f}{\partial z} + MR_d W_d \frac{C_d}{C_f}\left[r_{di} - r_f\right] \qquad (6)$$

The additional terms from equation 2 can be retained where the data warrant.

4.*3 Steady-state Sr isotope Model; retardation and near surface Sr isotope values*

The overall decrease of the pore fluid $^{87}Sr/^{86}Sr$ ratio with depth in the core is inferred to be a consequence of downward percolation of pore fluids coupled with dissolution of solid phases in the sediment. The interpretation of the pore water Sr isotopic profile depends on, among other things, whether the profile represents a steady state, which in turn depends to a significant degree on the likely pore fluid velocity. To proceed in analyzing the data, we first determine the implications for the percolation flux under the assumption that the Sr isotopic profile is at steady state and dispersion is negligible. Then we explore the effects of relaxing the steady state assumption, and also include the effects of dispersion. An important component of the analysis is recognizing

that the upper part of the Hanford Formation was deposited only about 13,000 years ago and hence the hydrologic system in that part of the section (to a depth of approximately 20 meters) is no older than that.

If the strontium profile represents a steady-state condition, then the differential form for the depth dependence of the pore fluid $^{87}Sr/^{86}Sr$ (denoted $r_f(z)$), is:

$$\frac{dr_f(z)}{dz} = \frac{MR_d W_d C_d}{vC_f}\left[r_d(z) - r_f(z)\right] \tag{7}$$

The validity of the steady-state approximation can be evaluated according to the characteristic time for an exchange front to traverse the system:

$$\tau = \frac{LK_{ret}}{v} \tag{8}$$

The retardation factor for Sr in Hanford sediments ranges from 80 to 240 based on K_d values of 5 to 15 mL/g (for sediment/porefluids with similar mineralogical, particle size, and chemical properties) and a bulk density of 1.9 g/mL [*Kincaid et al.*, 1998]. For the 299-W22-48 core, the pore fluid Sr content is known reasonably well from the distilled water leach data, but the amount of adsorbed Sr is not known precisely. A more specific estimate can be made from the data obtained by leaching the soil samples with ammonium acetate. The ammonium acetate extracted an average of 0.015 meq Sr/100 g soil [*Serne et al.*, 2002*b*]. Using the ammonium acetate values in conjunction with formation averages for the distilled water leaches results in formation-specific values for

K_{ret} of 104 to 138, with an average of 118. These values may be skewed to the upper range due to dissolution of carbonate by ammonium acetate.

Given a pore velocity of ca. 10 cm/yr, the time for the 18 m profile of the upper Hanford Formation to reach steady state is approximately 1800 years for a K_{ret} of 10 and about 20,000 years for K_{ret} equal to 120. Hence, the upper part of the Hanford Formation could be close to steady state even if the high values of K_{ret} are applicable. The deeper sediments are considerably older. Estimates range from several hundred thousand years old to several million years old for the deeper deposits of the Ringold Formation, [*Lindsey et al.*, 1994]. Geologically, there may be complications on time scales of 10,000 years or more due to the intermittent flooding and variable climate. It is hypothesized that the entire area covered by Hanford Formation sediments was under water for at least a brief time (less than 5 days) at ca. 13,000 years ago [*Chatters and Hoover*, 1994]. After the floodwaters drained away, the Columbia River may have had a significantly higher base level with periodic flooding, and hence groundwater may have been closer to the surface. Also, the river base level may have declined due to erosion, and the water table may have receded accordingly.

4.4 Estimation of the dissolution rate for the Hanford Sediments

The Hanford Site sediments are broadly granitic or granodioritic in composition. The primary minerals are quartz and two feldspars, with plagioclase much more abundant than alkali feldspar (Table 1a). Although a reliable in-situ method for measuring the weathering rates of sediments is not available, the bulk weathering rates for these sediments can be estimated based on a study of weathering rates for similar soils derived

from granitic terrains in California [*White et al.*, 1996]. *White et al.* [1996] analyzed alluvial soils of 0.2 ky-3000 ky age from the Merced chronosequence. The soils in the Merced area are formed on alluvial fan and terrace surfaces covered by grassland vegetation. The mean annual precipitation is 300 mm yr^{-1}, which falls primarily in the winter months. Enough similarities existbetween the Merced and the Hanford soils to suggest that the estimated weathering rates are comparable between the two sites (see Table 1a).

Weathering rates for the two primary Sr-bearing minerals in the Hanford sediments, plagioclase and alkali feldspar, can be calculated based on the chemical and isotopic data of *White et al.* [1996]. For the lower portion of the core (6-72 meters), the weathering rates for plagioclase and alkali feldspar, corresponding to the rough age of the sediments, are estimated to be between $10^{-6.0}$ to $10^{-5.5}$ yr^{-1} and $10^{-5.9}$ to $10^{-6.4}$ yr^{-1}, respectively. Weathering rates in the Merced chronosequence were also found to decrease by approximately $10^{-1.5}$ over timescales of approximately 300 ky [*White et al.*, 1996*; Bullen et al.*, 1997]. Similar age-dependent decreases in weathering rates over time have been demonstrated in other situations [*Hodson et al.,* 1998]. In addition, the weathering rates in the top few meters of a weathering profile are in general 2 to 3 times greater than for the lower portions; therefore the weathering rates for the younger sediments, comprising the top 6 meters of the profile at the Hanford Site, are likely to be slightly higher than for the remainder of the profile ($10^{-4.9}$ yr^{-1} and $10^{-5.17}$ yr^{-1} for plagioclase and K-feldspar respectively) [*White et al.*, 1996*; Hodson et al., 1998]*.

The bulk weathering rates for the column are estimated based on the average mineralogy and age of the sediment, assuming that quartz has a negligible contribution to

the Sr budget. Additional uncertainty is included in the formation-specific estimates to account for the effect of slightly larger annual precipitation at the Merced study site [*Stewart et al.,* 2001]. The estimated rates for the Hanford Site sediments are summarized in Table 4.

The weathering rate for biotite is much higher (approximately $10^{-2.3}$ yr^{-1}) than for the other minerals. Given the low concentration of Sr in biotite, the low relative abundance of biotite in the sediment, and its high $^{87}Sr/^{86}Sr$ ratio, the contribution of biotite to the bulk weathering rate is negligible for most of the section. However, as noted above, in the shallowest and youngest sediments, the biotite contribution may be significant.

4.5 Steady state model results

A steady-state finite difference model was constructed using Equation (7). C_d is assumed to be equal to 325 ppm — the average total Sr concentration of the bulk sediment samples that were measured. C_f and r_f are the measured values for the pore fluid at depth z (Table 2, columns 5 and 3, respectively). The value of the isotopic ratio for the bulk dissolving solid (r_d) is imprecise because of the considerable differences in the weathering rates, combined with the substantial variation in the $^{87}Sr/^{86}Sr$ ratio of the individual minerals. The model is calculated assuming that r_d is the value of the nitric acid leach for the corresponding depth. As discussed previously, the nitric acid leaches represent for Sr the most easily dissolved phases, with some contribution from exchangeable Sr as well. It is clear from the profile in Figure 4, and the mineral separates data that the nitric acid leach provides a reasonable approximation to the isotopic composition of the weathering material because it reflects the contribution of high-

$^{87}Sr/^{86}Sr$ from biotite (or another source), coupled with the larger contribution of lower-$^{87}Sr/^{86}Sr$ from the abundant feldspar minerals. Where the pore water Sr isotopes are elevated (e.g. 17.8 and 38.4 m), these spikes are preceded by concurrent increases in the Sr isotope ratios of the nitric acid leaches. Furthermore, the only possible means of fitting the model to the measured data for the top few meters of the core is through the nitric acid leach values since both the bulk sediment and average feldspar values would be less than the peak values occurring in the 3-5 m range. Near the surface, where the $^{87}Sr/^{86}Sr$ values increase rapidly, the weathering rate must be high to fit the pore water data. This is consistent with the previous discussion regarding rapid weathering at the surface where the sediment is younger, and physical and chemical weathering processes (with biological enhancement) are likely to be most effective.

The model was fit to the data by assuming a constant weathering rate for each formation and selecting the flux to minimize the misfit between r_f(model) and r_f (measured), while allowing the ratio of R_d/v_f to vary according to the water content. The model was fit to a smoothed general trend of the data such that the high-$^{87}Sr/^{86}Sr$ aberrations receive less weight than points lying along the general trend of the data. Given the heterogeneous nature of the Hanford sediments, these scattered spikes are most likely due to local variations in the mineralogy and perhaps an increased abundance of biotite, as the peaks do not appear to be correlated with changes in grain size or water content.

The best-fit scenario for the infiltration flux (7 ±3 mm/yr) and the corresponding values for R_d are shown in Figure 5a. The weathering rates required to fit the data for a range of infiltration fluxes, along with the broad estimates from the *White et al.*, [1996]

data are shown in Figure 5b. Given an order of magnitude change in the infiltration rate, the weathering rates must change by a similar magnitude. For the case of less than 0.1 mm/yr of infiltration, the weathering rates are exceedingly small, suggesting that the lower bound for infiltration must be approximately 4 mm/yr. An order of magnitude increase in the infiltration rate would not only require a weathering rate that is significantly greater than what is reported in the literature, but would also suggest that infiltration rates are close to 50% of the mean annual precipitation, which is unlikely for this semi-arid climate.

The effect of varying the value of r_d was also considered, starting at a depth of 4.5 meters. In order to fit the data, the infiltration flux must increase for any decrease in the value selected to represent the $^{87}Sr/^{86}Sr$ influx (r_d). The largest value for the infiltration flux (12.1 ± 2 mm/yr) corresponds to an r_d value of the bulk plagioclase equal to 0.7055. If the value of the bulk sediment is chosen (~0.711), a value of 9.2 ± 2 mm/yr is estimated, and finally for the nitric acid leach values, which are thought to represent the bulk exchangeable plus any readily dissolvable phases, the corresponding value is 7.0 ± 3 mm/yr. The important feature of these three estimates is that the values are not greatly different. Changing the value of r_d does not materially affect the inferred infiltration flux estimate. Given the considerable range of recharge estimates available for the 200 Areas (see Table 6), the range of infiltration flux values inferred here is small.

In the extreme case, where r_d is precisely equal to r_f, then the inferred infiltration flux would be zero. This possibility cannot be completely rejected, but we consider it to be highly unlikely. The major Sr-bearing minerals in the soils are feldspars, which have quite low $^{87}Sr/^{86}Sr$ values, and the bulk soil $^{87}Sr/^{86}Sr$ values are also significantly

different from, and lower than, the pore water values. There is a significant possibility that the $^{87}Sr/^{86}Sr$ of the Sr weathering flux is lower than the nitric leach values, but since the amount of Sr with high $^{87}Sr/^{86}Sr$ values in the soils must be very small, and feldspars must be undergoing some weathering, there is little likelihood that the bulk weathering flux has $^{87}Sr/^{86}Sr$ as high as that in the pore fluids. This conclusion applies mainly to the upper 40 to 45 m of the core; in the lower parts of the section, it is possible that the weathering flux $^{87}Sr/^{86}Sr$ is similar to the pore water values.

4.5 Effects of a non-steady state profile on the inferred recharge flux

The pore fluid $^{87}Sr/^{86}Sr$ values decrease most profoundly in the first 20 meters of the profile. These sediments, as discussed previously, were emplaced episodically over the past 10,000 to 15,000 years during catastrophic flood events. Assuming that the infiltration flux is on the order of several millimeters a year, the time required for the top 20 meters to reach equilibrium is less than or similar to the age of the sediments, thus calling into question the steady-state assumptions used in the determination of the infiltration flux values. In order to fully evaluate the effect of non-steady state hydrology on the Sr isotopic profile, a non-steady state numerical model was constructed using the simplified isotopic transport equation derived previously in equation (6).

A finite difference approximation was used to model the evolution of the Sr profile over a 15 ky period. The model considers the depth interval spanning from approximately 5 m to 70 m, the range over which the core is presumed to be unaffected by recent anthropogenic perturbations. The initial pore water $^{87}Sr/^{86}Sr$ ($t = 0$) value for the model is set at 0.714, similar to the Columbia River, which drains a region

comparable to the provenance of the catastrophic flood waters that once inundated the Hanford Formation. It is assumed that the initial pore water is dilute in Sr and reflects the average value of the residual floodwaters, which presumably saturated the sediments for a period of time after the initial deposition of the Hanford Formation. Fluid entering the model at the surface is given an initial Sr ratio equal to the pore water value of 0.721 measured at 4.5 meters depth.

For this numerical model, the Sr isotopic profiles were allowed to evolve over a 15,000-year timescale and no fitting parameters other than the documented model parameters were used to guide the evolution of the profile. The timescale was chosen to represent the estimated age of the upper Hanford Formation. Several different scenarios are considered based on the uncertainty of the principal parameters: v, K_{ret} and r_d. The remaining parameters in equation (6) were either selected from previous hydrologic models at the Hanford site or from the steady-state model results previously described.

The model parameters used in each scenario are presented in Table 5. Several simplifying assumptions are made in the formulation of the numerical model. Pore water (C_f) and dissolving solid (C_d) Sr concentrations as well as the $^{87}Sr/^{86}Sr$ values of the dissolving solid are assumed to be constant over time and depth. Dissolution rates (R_d) and infiltration fluxes are also held constant within each model scenario. An initial sensitivity test indicated that the model results were insensitive to changes in the weathering rate (R_d) over the magnitude of estimates for the Hanford sediments (Table 4), therefore a depth-averaged value was assigned. The model was also relatively insensitive to changes in the ratio of C_d to C_f for the range measured in the initial data, so the average value for each parameter was used in the model. The value of the dispersivity (λ) was set

to 7 m based on previous studies of vadose zone transport at the Hanford Site [*Mann et al.*, 1997]. The range of values for K_{ret} (3 to 118) was chosen based on the previous discussion of the retardation factor for the 299-W22-48 borehole and other independent estimates of K_d for uncontaminated waters at a site proximal to the 200 West area.

The first model investigates the effect of variations in the infiltration flux and the retardation factor while all other parameters are held constant (Model 1). The infiltration fluxes and K_{ret} values represent the range of possible conditions. The first profile (1a) represents the results from the steady-state model using the value for the retardation factor estimated for the 299-W22-48 core.

For Model 2, the $^{87}Sr/^{86}Sr$ ratio for the dissolving solids was considered over a range of possible values: average plagioclase ratio, average bulk sediment, and the ratio of the high-end weathering flux (0.718). This last scenario reflects the potential for a small but highly reactive radiogenic $^{87}Sr/^{86}Sr$ phase to control the pore fluid composition in the first 15,000 years of weathering.

4.6 Non-steady State Model Results

The results of the two model scenarios plotted against the measured $^{87}Sr/^{86}Sr$ pore water ratios are shown in Figure 6. In each plot, the 15,000 year-old profile is shown. For most cases the shape of the model profile is markedly similar to the general trend of the measured pore water isotopic data.

In Model 1, the effect of changes in the infiltration flux and retardation factor are illustrated— the location of the high -$^{87}Sr/^{86}Sr$ front, and the gradient of the Sr isotope values, change according to the value of q and K_{ret}. For a low infiltration rate and low

retardation factor (Model 1c) the center of the front has propagated to about 15 meters and the profile approaches steady state. The comparatively small flux combined with the minimal retardation factor demonstrates the balance between rapid exchange and slow transport. A doubling of the q value and a high K_{ret} in Model 1d produces a similar profile to Model1b, where the center of the front has advanced to approximately 30 meters in both cases.

As shown in Models 1a and 1b, the value selected for the retardation factor changes the gradient in the $^{87}Sr/^{86}Sr$ values for a corresponding infiltration flux. The assumption of a linear isotherm, which is common in most groundwater models, may also affect the propagation of the exchange front because in regions of the core with high pore water cation concentrations, such as the calcareous lower Cold Creek layer, the competition of other cations for the exchange sites lowers the Sr K_d value. This would in effect decrease the Sr K_d value and cause the Sr to advance at a greater rate. The tendency of the model to over or underestimate the $^{87}Sr/^{86}Sr$ profile suggests that the K_d values may differ slightly between each unit.

Model 2 and Model 1a demonstrate the effect of changes in the isotopic composition of the dissolving material (r_d). The profiles are governed by mixing of the initial pore water with the percolating water, which is in turn controlled by the value of r_d and the weathering rate. With depth, the $^{87}Sr/^{86}Sr$ values of the pore water approach the value of the dissolving solid, and over time or with rapid transport, as shown in 1c, the values will reach a steady state profile. A change in either the infiltration flux or the retardation factor would alter the slope of the profile either away from or towards the actual values, as portrayed in the first model.

4.7 Constraints on the infiltration flux estimates

There are two parameters in the model that control the magnitude of the infiltration flux, the isotopic value of dissolution flux, r_d, and the value of the bulk weathering rate, R_d. In order to understand how accurate the infiltration flux estimates are, it is instructive to look at the effect of changing r_d and R_d. The first possibility is that r_d is equal to r_f, in which case there would be no infiltration at the site and the weathering rate would have to be extremely low ($<10^{-9}$ yr^{-1}), which is a highly unlikely scenario given the Sr concentrations in the pore fluids. Furthermore, the nitric acid leach data and bulk sediment data indicate that the isotopic ratio of the dissolving solid is not equal to or greater than the pore fluid ratio, thus the minimum infiltration flux, even if r_d is greater than the $^{87}Sr/^{86}Sr$ of the nitric acid leach, will still be on the order of several millimeters per year. Conversely, the upper-bound infiltration flux is well constrained by setting r_d equal to the bulk plagioclase value, since it is unlikely that weathering of any other minor mineral, such as $CaCO_3$ could result in a flux of the $^{87}Sr/^{86}Sr$ ratio lower than the plagioclase value. Given the low abundance of $CaCO_3$ in the majority of the sediments (<1.5 wt%), the only region where carbonate weathering would contribute to r_d would be in the CCUc-f(calc) layer. However, Sr isotopes do not fractionate measurably during the precipitation of secondary minerals, therefore it is unlikely that carbonate, even in the CCUc-f(calc) layer, would contribute any Sr that is significantly different from the bulk sediment or average plagioclase composition.

The model results suggest that the infiltration flux values of 5 to 10 mm/yr encompass the maximum range of possible values. While alterations in both the K_d and the r_d values can produce dramatic changes in the slope of the $^{87}Sr/^{86}Sr$ profile, using the

estimates based on the data from the 299-W22-48 core yields estimates of the infiltration rate that are in general agreement with site-wide estimates. Further work should be done to understand the exchange properties of Sr in the Hanford sediments and how the mineralogy and weathering rate influences the Sr signature of the pore waters. In addition, determination of the actual $^{87}Sr/^{86}Sr$ ratio of the dissolving solid and how this changes over the age of the sediment, will greatly increase the potential of this application to other vadose zone sites.

5. CONCLUSIONS

The majority of recharge estimates for the 200 Areas and the entire Hanford Site have been made using either lysimeters, numerical models, or for undisturbed sites, natural tracer (e.g., Cl mass balance) methods. The existing data for the site are summarized in Table 6. In addition, tracer data for an undisturbed, vegetated site near the 200 West Area, where the 299-W22-48 borehole is located, suggests the infiltration flux to be on the order of 0.01 to 0.03 mm/yr [*Fayer et al.,* 2000]. Numerical modeling attempts suggest that the infiltration flux in the 200 Areas is on the order of 3 mm/yr [*Fayer et al.*, 1995], while *Bauer and Vaccaro* [1990] estimate the site-wide flux to be 1.2 to 12.7 mm/yr. Numerous researchers also suggest that removal of vegetation may dramatically increase infiltration rates. Plant uptake may be on the order of 50 to 75% of precipitation, and when combined with evaporation, may result in negligible infiltration rates [*Or and Rubin*, 1993]. This effect in part explains the highly variable nature of infiltration rates measured at the Hanford site.

The results from the Sr method employed in this study provide an estimate of infiltration flux that most likely represents an average value that applies to the past 1000 to 10,000 years. This averaging is provided by the relatively large inventory of adsorbed Sr held in the soil column (cf. *Johnson and DePaolo*, 1997b). The fact that we can derive a long-term average value for the natural fluid flux may be useful in modeling the future performance of the site for regulatory purposes; where projections out to thousands of years into the future may be required.

Due to the heterogeneous grain size distribution and highly variable climate during the Holocene, it is unlikely that the infiltration flux is constant either temporally or spatially. Given the range of infiltration estimates from this study (7.0 mm/yr to 12 mm yr^{-1}), the resulting transit time for water from the surface to the water table is in the range of 600-1900 years. This estimate is valid only for meteoric water that is percolating downward from the surface and does not apply to point discharges because this method assumes that there is no hydraulic gradient in lateral directions. This distinction is important because leak simulations at the Hanford site have found significant lateral spreading to occur as a result of natural capillary barrier effects [*Ward and Gee*, 2000.]

The other physical parameter that appears to have the strongest effect on infiltration at the site is the nature of the surface sediments, either loam or sand. Infiltration rates for a coarse-grained un-vegetated soil can be on the order of 50% of the precipitation, or approximately 80 mm/yr for the Hanford Site. Values of this magnitude are seldom measured, most likely because winter precipitation is stored in the finer-grained surface soils and inter-bedded silt or clay lenses and then utilized by plants or

evaporated during the dry season. The data for this site suggest that evaporative processes can remove on the order of 90% of precipitation.

One advantage of the Sr isotope measurements over the lysimeter studies is that they do not cause any disturbance prior to measurement, hence preferential paths in the soil structure are captured in the Sr isotopic method. Tracer studies such as ^{137}Cs, ^{3}H, and Cl are limited by both the textural nature of the soils and the degree of prior chemical and physical disturbance at the site and thus are often not amenable to coarse-textured or engineered sites [*Mann et al.*, 1997; *Tindall and Kunkel*, 1999].

For groundwater and weathering studies using Sr isotopes, this work further elicits the importance of considering the $^{87}Sr/^{86}Sr$ ratios of the individual minerals in the parent material, particularly for granite-derived soils or sediments where the weathering rates and isotopic compositions may vary dramatically between minerals. As seen in the top few meters of the core, a small region with substantially different Sr isotopes can effect a large portion of the profile. Further work should be done to quantify the true value of r_d for heterogeneous sediments and how this value might change with sediment age and composition.

If the isotopic flux (R_d and r_d) derived from the weathering of the sediments can be reasonably estimated, then measurements of the pore fluid $^{87}Sr/^{86}Sr$ values can offer another method for deriving an estimate of long-term infiltration flux for a deep vadose zone composed of extremely heterogeneous sediments. The ratio of the weathering rate (R_d) to the pore fluid velocity (v) can then be calculated based on measurements of the isotopic values of the pore fluid. The method is quite versatile and has great potential at contaminated sites where other isotopic methods for evaluating recharge such as ^{3}H and

^{36}Cl techniques may be complicated by on-site contamination. In addition, the ability to make long-term *in situ* measurements of infiltration rates can be advantageous when coupled with other physical and geochemical measurements.

Acknowledgements

We would like to acknowledge Tom Owens and Julia Bryce for their assistance in the laboratory and Evan Dresel and John Evans at PNNL for help in obtaining samples and for providing site information. Funding was provided by the Department of Energy under contract DE-AC06-76RL01830 through the Hanford Science and Technology Program, and by the Director, Office of Science, Basic Energy Sciences, Chemical Sciences, Geosciences and Biosciences Division of the U.S. Department of Energy under Contract No. De-AC03-76SF00098.

6. REFERENCES

Baker, D.R., Tracer versus trace element diffusion —diffusional decoupling of Sr concentration from Sr isotope composition. *Geochimica et Cosmochimica Acta, 53*, 3015-3023, 1989.

Bauer, H.H. and J.J. Vaccaro, Estimates of ground water recharge to the Columbia Plateau Regional Aquifer System; Washington, Oregon and Idaho for predevelopment and current land use conditions, U.S. Geological Survey, Tacoma, Washington, *WRIR 88-4108*, 1990.

Blum, J. D., and Y. Erel, A silicate weathering mechanism linking increases in marine Sr-87/Sr-86 with global glaciation. *Nature*, 373(6513), 415-418, 1995.

Blum, J. D., and Y. Erel, Rb-Sr Isotope Systematics of a Granitic Soil Chronosequence: The Importance of Biotite Weathering, *Geochimica et Cosmochimica Acta, 61*, 3193-3204, 1997.

Brodeur, J.R., C.J. Koizumi, J.F. Bertsch, Vadose Zone Characterization Project at the Hanford Tank Farms: SX Tank Farm Report, *DOE/ID/12584—268*, 1996.

Bullen T.D., D.P Krabbenhoft, and C. Kendall, Kinetic and mineralogic controls on the evolution of groundwater chemistry and $^{87}Sr/^{86}Sr$ in a sandy silicate aquifer, Northern Wisconsin, USA, *Geochimica et Cosmochimica Acta*, *60,* 1807-1821, 1996.

Bullen T. D., A. F. White, A. E. Blum, J. W. Harden, M. S. Schulz, Chemical weathering of a soil chronosequence on granitoid alluvium. II. Mineralogic and isotopic constraints on the behavior of strontium, *Geochimica et Cosmochimica Acta*, *61*, 291-306, 1997.

Campbell, M.D., G.W. Gee, Water balance lysimetry at a nuclear waste site. Proceedings of the International Symposium on Lysimetry (R.G. Allen, ed.). *Amer. Soc. Civil. Engr.*, 125-132, 1991.

Chatters J.C and K.A. Hoover, Response of the Columbia River fluvial system to Holocene climate change, *Quaternary Research, 37*, 42-59, 1992.

Conrad, M.E., D.J. DePaolo, K. Maher, G.W. Gee, A.W. Ward, The impact of sedimentary layering on water and chemical transport in the Hanford vadose zone, submitted to Water Resources Research, August, (MS 1668), 2002.

DePaolo, D.J, M.E. Conrad, K. Maher, and G.W. Gee, Oxygen and hydrogen isotopes in pore fluids from a 70m-thick vadose zone soil section at Hanford, Washington: Implications for recharge and horizontal fluid movement, submitted to Vadose Zone Journal, August, 2002.

Dickin, A.P., *Radiogenic Isotope Geology*, Cambridge University Press, New York, NY, 1995.

Fayer, M.J. and M.B. Walters, Estimated recharge rates at the Hanford Site. Pacific Northwest National Laboratory, Richland, Washington, *PNL-10285,1995.*

Fayer, M.J., E.M. Murphy; J.L. Downs; F.O. Khan, C.W. Lindenmeier, and B.N. Bjornstad, Recharge data package for the Immobilized Low-Activity Waste 2001 Performance Assessment. Pacific Northwest National Laboratory, Richland, Washington, *PNNL-13033*, 2000.

Gee, G.W., Fayer M.J., Rockhold, M.L., and M.D. Campbell, Variations in recharge at the Hanford Site, *Northwest Science*, *66,* 237-250, 1992.

Hartman, M.J. (ed),. Hanford Site groundwater monitoring for fiscal year 1998. Pacific Northwest National Laboratory, Richland, Washington, *PNNL-12086*, 1998.

Hodson M.E., S.J. Langan, F.M. Kennedy, and D.C. Bain, Variation on soil surface area in a chronosequence of soils from Glen Feshie, Scotland and its implications for mineral weathering rate calculations, *Geoderma*, 85, 1-18, 1998.

Hooper, P.R. and C.J. Hawkesworth, Isotopic and geochemical constraints on the origin and evolution of the Columbia River Basalt, *J. Petrol.*, *34*, 6, 1203-1246, 1993.

Johnson, T. M., and D. J. DePaolo, Interpretation of isotopic data in groundwater-rock systems: model development and application to Sr isotopic data from Yucca Mountain, *Water Resources Research, 30*, 1571-1587, 1994.

Johnson, T. M., and D. J. DePaolo, Rapid exchange effects on isotope ratios in groundwater systems, 1. Development of a transport-dissolution-exchange model, *Water Resources Research*, *33*, 187-195, 1997a.

Johnson, T. M., and D. J. DePaolo, Rapid exchange effects on isotope ratios in groundwater systems, 2. flow investigation using Sr isotope ratios, *Water Resources Research*, *33*, 197-205, 1997b.

Johnson, T., R. C. Roback, T. L. McLing, T. D. Bullen, D. J. DePaolo, C. Doughty, R. J. Hunt, R. W. Smith, L. D. Cecil, and M. T. Murrell, Groundwater "fast-paths" in the Snake River Plain Aquifer: radiogenic isotope ratios as natural groundwater tracers," *Geology, 28*, 871-874, 2000.

Kincaid C. T., M. P. Bergeron, C. R. Cole, M. D. Freshley, N. L. Hassig, V. G. Johnson, D. I. Kaplan, R. J. Serne, G. P. Streile, D.L. Strenge, P. D. Thorne, L. W. Vail, G. A. Whyatt, and S. K. Wurstner, 1998. Composite analysis for low-level waste disposal in the 200 Areas Plateau of the Hanford Site, Pacific Northwest National Laboratory, Richland, Washington. *PNNL-11800*.

Lindsey, K.A., J.L. Slate, G.K. Jaeger, K.J. Swett and R.B. Mercer, Geologic setting of the low-level burial grounds. Westinghouse Hanford Company, Richland, Washington, *WHC-SD-TI-290*, 1994.

Mann, F.M., C.R. Eiholzer, Y. Chen, N.W. Kline, A.H. Lu, B.P. McGrail, P.D. Ritmann, Low-level tank waste interim performance assessment, *HNF-EP-0884*, 1997.

Murphy, E.M., T.R. Ginn and J.L. Phillips, Geochemical estimates of Paleorecharge in the Pasco Basin — Evaluation of the chloride mass balance technique. *Water Resources Research*. 32(9):2853-2868, 1996.

Or D., and Y. Rubin, Stochastic modeling of unsaturated flow in heterogeneous media with water uptake by plant roots — tests of the parallel columns model under 2-dimensional flow conditions. *Water Resources Research*, 29(12), 4109-4119, 1993.

Richter F.M. and D.J. DePaolo, Diagenisis and Sr isotopic evolution of seawater using data from DSDP 590B and 575, *Earth Planet. Sci. Lett., 90***,** 382-394, 1988.

Richter F.M., Fluid flow in deap sea carbonates – estimates based on porewater Sr. *Earth Planet. Sci. Lett., 119*, 133-141, 1993.

Rockhold, M.L., M.J. Fayer, G.W. Gee and M.J. Kanyid, Natural groundwater recharge and soil-water balance at the Hanford Site, Pacific Northwest National Laboratory, Richland, Washington, *PNNL-7215*, 1990.

Routson, R.C., M.R. Fuchs and W.A. Jordan, Recharge estimate for the Hanford Site 200 Areas Plateau. Westinghouse Hanford Company, Richland, Washington, *WHC-EP-0046,* 1988.

Routson, R.C. and V.G. Johnson, Recharge estimates for the Hanford Site 200 Areas Plateau. *Northwest Science,* 64(3):150-158, 1990.

Serne R.J., H.T. Schaef, B.N. Bjornstad, B.A. Williams, D.C. Lanigan, D.G. Horton, R.E. Clayton, V.L. LeGore, M.J. O'Hara, C.F. Brown, K.E. Parker, I.V. Kutnyakov, J.N. Serne, A.V. Mitroshkov, G.V. Last, S.C. Smith, C.W. Lindenmeier, J.M. Zachara, and D.B. Burke, Characterization of uncontaminated vadose zone sediment from the Hanford Reservation - RCRA borehole core samples and composite samples. Pacific Northwest National Laboratory, Richland, Washington, *PNNL-13757-1*, 2002a.

Serne R.J., H.T. Schaef, B.N. Bjornstad, D.C. Lanigan, G.W. Gee, C.W. Lindenmeier, R.E. Clayton, V.L. LeGore, M.J. O'Hara, C.F. Brown, R.D. Orr, G.V. Last, I.V. Kutnyakov, D.S. Burke, T.C. Wilson, and B.A. Williams, Geologic and geochemical data collected from vadose zone sediments from borehole 299 W23-19 [SX -115] in the S/SX Waste Management Area and preliminary interpretations. Pacific Northwest National Laboratory, Richland, Washington, *PNNL-13757-2, 2002b.*

Sonnenthal, E.L. and G.S. Bodvarsson. Constraints on the hydrology of the unsaturated zone at Yucca Mountain, NV from three-dimensional models of chloride and strontium geochemistry, *Journal of Contaminant Hydrology*, Volume 38, Issues 1-3, 1999, 107-156.

Stewart, B.W., R.C. Capo, and O.A. Chadwick. Effects of rainfall on weathering rate, base cation provenance, and Sr isotope composition, *Geochimica et Cosmochimica Acta, 65,* 1087-1099, 2001.

Stormont, J.C., C.E. Anderson, ASCE Members, Capillary barrier effect from underlying coarser soil layer. *Journal of Geotechnical and Geoenvironmental Engineering.* 125: 641-648, 1999.

Taylor, S.T., J.D. Blum, A.C. Lasaga, and I.N. MacInnis, Kinetics of dissolution and Sr release during biotite and phlogopite weathering. *Geochimica et Cosmochimica Acta, 64,* 1191-1208, 2000a.

Taylor, S.T., J.D. Blum, A.C. Lasaga, The dependence of labradorite dissolution and Sr isotope release rates on solution saturation state. *Geochimica et Cosmochimica Acta*, *64* (N14), 2389-2400, 2000b.

Tindall, J.A. and J.R. Kunkel, *Unsaturated Vadose Zone Hydrology for Scientists and Engineers.* Prentice Hall, Saddle River, NJ., 1999.

US DOE, Final environmental impact statement: Disposal of Hanford defense high-level transuranic and tank wastes, Hanford Site, Richland, Washington. U.S. Department of Energy, Washington, D.C., *DOE/EIS-0113*, 1987.

US DOE, Standardized stratigraphic nomenclature for Post-Ringold Formation Sediments within the Central Pasco Basin. Department of Energy, Richland Operations, Richland, Wa., *DOE/RL-2002-39*, 2002

Ward, A.L., T.G. Caldwell, G.W. Gee, Vadose Zone Transport Field Study: Soil water content distributions by Neutron Moderation, Pacific Northwest National Laboratory, web report*, http://vadose.pnl.gov*, 2000.

White, A. F., A. E. Blum, M. S. Schulz, T. D. Bullen, J. W. Harden, and M. L. Peterson, Chemical Weathering Rates of a Soil Chronosequence on Granitic Alluvium: I. Quantification of Mineralogical and Surface Area Changes and Calculation of Primary Silicate Reaction Rates, *Geochimica et Cosmochimica Acta*, *60* (N14), 2533-2550, 1996.

Figure Captions

Figure 1. (a) Hanford Site map showing location of 200 Area plateau and the 299-W22-48 bore hole and other pertinent locations. (b) Schematic cross–section depicting the predominant direction of groundwater flow.

Figure 2. Lithology and Volumetric Water Content for the 299-W22-48 borehole. HFGD: Hanford Formation, gravel-dominated facies; HFSD: Hanford Formation, sand-dominated facies; CCUf(lam-msv): Cold Creek unit, silt and fine-grained sand; CCUc-f(calc): Cold Creek unit, calcic paleosol; Rtf: Ringold Formation, upper fines; Rwi: Ringold Formation, sandy gravel. (Data from *Serne et al.* [2002b] and *US DOE* [2002]).

Figure 3. Background geochemical data for 1:1 sediment to deionized water extracts. (a) pH data for 1:1 sediment to deionized water extracts. (b) Chemical data for water extracts (ICP measurements from *Serne et al.*, [2002a]).

Figure 4. (a) Theoretical pore water Sr concentrations (mg/L) and nitric acid leaches (ppm). (b) $^{87}Sr/^{86}Sr$ profiles for porewaters, nitric acid leaches and bulk sediment. Columbia river values (0.7137-0.7144) and the approximate location of the unconfined aquifer are shown for reference.

Figure 5. Steady State Model best-fit trajectory and Rd/v profile. (a) Best-fit trajectory corresponding to a dissolving solid 87Sr/86Sr ratio (rd) of the nitric acid leach value and infiltration flux of 7 mm/yr. (b) Weathering rates required to fit the data for various infiltration rates. The estimated weathering rates are shown for reference. An order of magnitude change in the infiltration flux mandates a comparable change in the infiltration rate in order to fit the pore water data.

Figure 6: Non-Steady State Model, $\theta = 0.09$ and $\lambda = 7$m for all cases. (a) The effect of changes in the infiltration flux and retardation factor,(K_{ret}). (b) Model trajectories showing the effect of changes in the value of r_d.

Table Captions

Table 1a: Average mineralogy of sediments for the Hanford Formation, Cold Creek unit, and the Ringold Formation (wt%) based on X-ray diffraction measurements. The mineralogy of the average parent material for Merced soils is shown for comparison.

Table 1b: Particle size distribution for the Hanford, Cold Creek, and Ringold Formations determined by dry sieve methods. $CaCO_3$ (% by weight) determined by coulometric titration (ASTM Procedure D-513) is also shown. (Data summarized from Serne et al., 2002a,b.)

Table 2: Volumetric water content and Sr isotopic data for the 299-W22-48 core (LBNL measurements).

Table 3: $^{87}Rb/^{86}Sr$ and $^{87}Sr/^{86}Sr$ values and chemical analysis results for mineral separates from selected depths.

Table 4: Weathering rates for the 299-W22-48 core. Weathering rates are calculated based on the average mineralogy and Sr content of each formation according to the weathering rates presented in *White et al.* [1996] and *Taylor et al.* [2000a, b].

Table 5: Model parameters for non-steady state model scenarios.

Table 6: Summary of estimated infiltration rates for Hanford sediments.

Table 1a: Average mineralogy of sediments for the Hanford Formation, Cold Creek unit, and the Ringold Formation (wt%) based on X-ray diffraction measurements. The mineralogy of the average parent material for Merced soils is shown for comparison.

Formation	Quartz	Plagioclase	K-feldspar	Other
Hanford: 12 m (HFSD1)[a]	60	20	<5	15
Hanford: 14 m (HFGD)	20	15	<5	15
Hanford: 28 m (HFSD2)	45	15	40	0
Cold Creek: 41.5 m (CCUf)	80	30	10	0
Cold Creek: 45 m (CCUc-f)	25	10	10-20	40 (Calcite)
Ringold: 50 m (Rtf)	65	10	20	10
Merced Soils (Average Mineralogy)[b]	33	33	16	18

[a]Hanford data from *Serne et al.* [2002a,b].
[b] Soils from *White et al.* [1997] shown for comparison.

Table 1b:Particle size distribution for the Hanford, Cold Creek, and Ringold Formations determined by dry sieve methods. $CaCO_3$ (% by weight) determined by coulometric titration (ASTM Procedure D-513) is also shown. (Data summarized from *Serne et al.*, [2002a,b].)

Formation	% Gravel	% Sand	% Silt/Clay	% $CaCO_3$
Hanford: 12 m (HFSD1)	1.4	89.9	8.78	1.7
Hanford: 14 m (HFGD)	73.8	23	3.6	2.3
Hanford: 28 m (HFSD2)	0.4	94.6	5.0	1.8
Hanford: 31 m (HFSD2)	.01	98.1	1.9	3.3
Cold Creek: 41.5 m (CCUf)	1.0	60.3	38.6	2.9
Cold Creek: 45 m (CCUc-f)	52.4	27.1	15.2	38.3
Ringold: 50 m (Rtf)	0	94.2	5.8	0.75

Table 2: Volumetric water content and Sr isotopic data for the 299-W22-48 core, (LBNL measurements).

Depth	Water Content	Pore Water Rinses			Nitric Acid Leaches		Bulk Sediment	
meters	θ	$^{87}Sr/^{86}Sr$	[Sr] μg/g soil	[Sr] mg/L[a]	$^{87}Sr/^{86}Sr$	[Sr] μg/g soil	$^{87}Sr/^{86}Sr$	[Sr] μg/g soil
0.4	0.094	0.7145	664.67	12.73	0.7127	31.10	0.7095	
1.9	0.177	0.7153	75.02	0.76	0.7163	41.96	0.7115	
3.0	0.168	0.7205	41.11	0.44	0.7191	29.46	0.7113	
4.5	0.148	0.7210	7.75	0.09	0.7165	30.38		
6.0	0.134	0.7203	37.11	0.50	0.7165	29.70		
7.5	0.044	0.7191	23.93	0.98	0.7109	21.29		
9.1	0.172	0.7200	41.28	0.43	0.7135	29.47		
10.6	0.061	0.7182	26.41	0.78	0.7109	25.22		
12.1	0.124	0.7178	75.02	1.08	0.7129	30.68		357.7*
13.6	0.051	0.7177	33.67	1.19	0.7123	21.57		310.7*
15.3	0.094	0.7179	69.39	1.32	0.7137	21.33	0.7112	351.3
17.0	0.073	0.7177	67.88	1.67	0.7142	23.64		
17.1	0.067	0.7193	72.74	1.96	0.7140	28.03		
17.6	0.060	0.7178	70.74	2.14	0.7148	24.75		
19.0	0.041	0.7176	38.30	1.69	0.7141	22.77		
21.3	0.034	0.7165	20.28	1.07	0.7149	25.43		
24.3	0.054	0.7165	75.02	2.50	0.7139	27.87		
26.4	0.096	0.7153	52.40	0.98	0.7138	27.97	0.7114	279.2
29.4	0.209	0.7150	90.48	0.78	0.7147	31.63		342*
32.6	0.061	0.7145	49.79	1.46	0.7131	27.92	0.7109	215.3
36.7	0.080	0.7157	53.63	1.21	0.7114	31.22		
38.0	0.069	0.7142	42.94	1.12	0.7123	30.52	0.7105	
38.4	0.060	0.7177	108.02	3.24	0.7127	29.31	0.7113	
44.7	0.430	0.7145	133.99	0.56	0.7106	197.36	0.7107	332*
45.4	0.178	0.7153	75.02	0.76	0.7163		0.7107	294
46.2	0.038	0.7138	100.12	4.74	0.7133	25.73		
50.0	0.045	0.7137	52.74	2.11	0.7129	17.97		264*
51.2	0.213	0.7153	71.66	0.61	0.7132	22.42		
52.0	0.065	0.7131	31.23	0.87	0.7164	17.40		
53.8	0.057	0.7131	31.23	0.98	0.7158	11.98		
57.2	0.054	0.7123	17.14	0.57	0.7135	12.17		
71.8	0.253	0.7102	13.03	0.09	0.7131	18.06		

[a]Theoretical pore water Sr concentrations calculated from wt. % water in soil.

* XRF measurements from *Serne et al.,* 2002a.

Table 3: $^{87}Rb/^{86}Sr$ and $^{87}Sr/^{86}Sr$ values and chemical analysis results for mineral separates from selected depths.

Mineral	Depth (m)	[K] (wt %)	[Rb] (ppm)	[Sr] (ppm)	$^{87}Rb/^{86}Sr$	$^{87}Sr/^{86}Sr$
Biotite (HFSD1)	0.4	3.12	267.83	192.22	4.03	0.71083
Biotite (HFSD1	8.8	0.14	280.39	75.11	10.80	0.71812
Biotite (HFSD1)	10.4	3.23	193.70	72.09	7.78	0.71150
Biotite (HFSD2)	21.0	3.16	292.70	53.81	15.74	0.71895
Biotite (HFSD2)	37.8	2.94	215.81	91.93	6.79	0.71397
Plagioclase (HFSD1)	0.3	ND	95.14	2315.60	0.12	ND
Plagioclase (HFSD1)	2.7	0.55	14.30	155.15	0.27	0.70495
Plagioclase (HFSD1)	8.8	0.18	4.47	156.43	0.08	0.70487
Plagioclase (HFSD1)	10.4	0.46	15.93	372.97	0.12	0.70467
Plagioclase (HFSD2)	21.0	1.77	68.65	501.37	0.40	0.70753
K-Feldspar (HFSD1)	0.3	2.13	84.99	238.72	1.03	0.70615
K-Feldspar (HFSD1)	2.7	1.91	53.95	217.00	0.72	0.70773
K-Feldspar (HFSD1)	8.8	2.04	77.45	352.41	0.64	ND
K-Feldspar (HFSD1)	10.4	2.15	42.26	336.96	0.36	0.70603
K-Feldspar (HFSD2)	21.0	2.95	106.06	326.42	0.94	0.70982

ND: not determined due to insufficient sample.

Table 4: Weathering rates for the 299-W22-48 core. Weathering rates are calculated based on the average mineralogy and Sr content of each formation according to the weathering rates presented in *White et al.* [1996] and *Taylor et al.* [2000a, b].

Formation	Depth Interval (m)	Weathering Rate (yr^{-1})
Hanford (HFSD1)	0-12	$10^{-6.0}$-$10^{-5.4}$
Hanford (HFGD)	12- 19	$10^{-7.1}$- $10^{-6.1}$
Hanford (HFSD2)	19-38	$10^{-6.8}$- $10^{-5.8}$
Palouse: (PPLz)	38-44.5	$10^{-6.7}$- $10^{-5.78}$
Palouse: (PPLc)	44.5-45.4	$10^{-7.0}$- $10^{-6.05}$
Ringold: (Rtf)	45.4-70	$10^{-7.0}$- $10^{-6.05}$
Merced Soils	NA	$10^{-6.4}$- $10^{-6.25}$

Table 5: Model parameters for non-steady state model scenarios.

Input Parameter	Model 1: effect of velocity and retardation on exchange front.				Model 2: effect of variable dissolution inputs.		
	1a	**1b**	**1c**	**1d**	**2a**	**2b**	**2c**
$r_f (z, t = 0)$	0.714	0.714	0.714	0.714	0.714	0.714	0.714
$r_f (z = 0, t > 0)$	0.721	0.721	0.721	0.721	0.721	0.721	0.721
$r_d (z)$	0.715	0.715	0.715	0.715	**0.705**	**0.711**	**0.718**
C_f *(ppm soil)*	0.073	0.073	0.073	0.073	0.073	0.073	0.073
C_d *(ppm soil)*	325	325	325	325	325	325	325
K_{ret}	118	**60**	**3**	**118**	118	118	118
□ *(mm/yr)*	7.3	7.3	**1**	**14**	**7.3**	**7.3**	**7.3**
$R_d (yr^{-1})$	$10^{-6.43}$	$10^{-6.43}$	$10^{-6.43}$	$10^{-6.43}$	$10^{-6.43}$	$10^{-6.43}$	$10^{-6.43}$

Table 6: Summary of estimated infiltration rates for Hanford sediments.

Method:	Site Description:	Infiltration rate:
Sr Isotope Method	299-W22-48 Core, 200-West	7 mm/yr
Stable Isotope measurements[a]	299-W22-48 Core, 200-West	2-8 mm/yr
Chloride Mass Balance[b]	Wye Barricade, Hanford	0.01 mm/yr
Lysimeter studies[c]	Bare Sand, 200-East	90 mm/yr
Lysimeter studies[d]	Sand/Tumbleweed, 200-East	< 2 mm/yr
Lysimeter studies[e]	Bare silt loam, FLTF[f]	0 mm/yr

[a]DePaolo et al , 2002
[b]Murphy et al., 1996.
[c]Rockhold et al., 1990
[d]Routson and Johnson, 1990.
[e]Campbell et al., 1991
[f]Field Lysimeter Test Facility

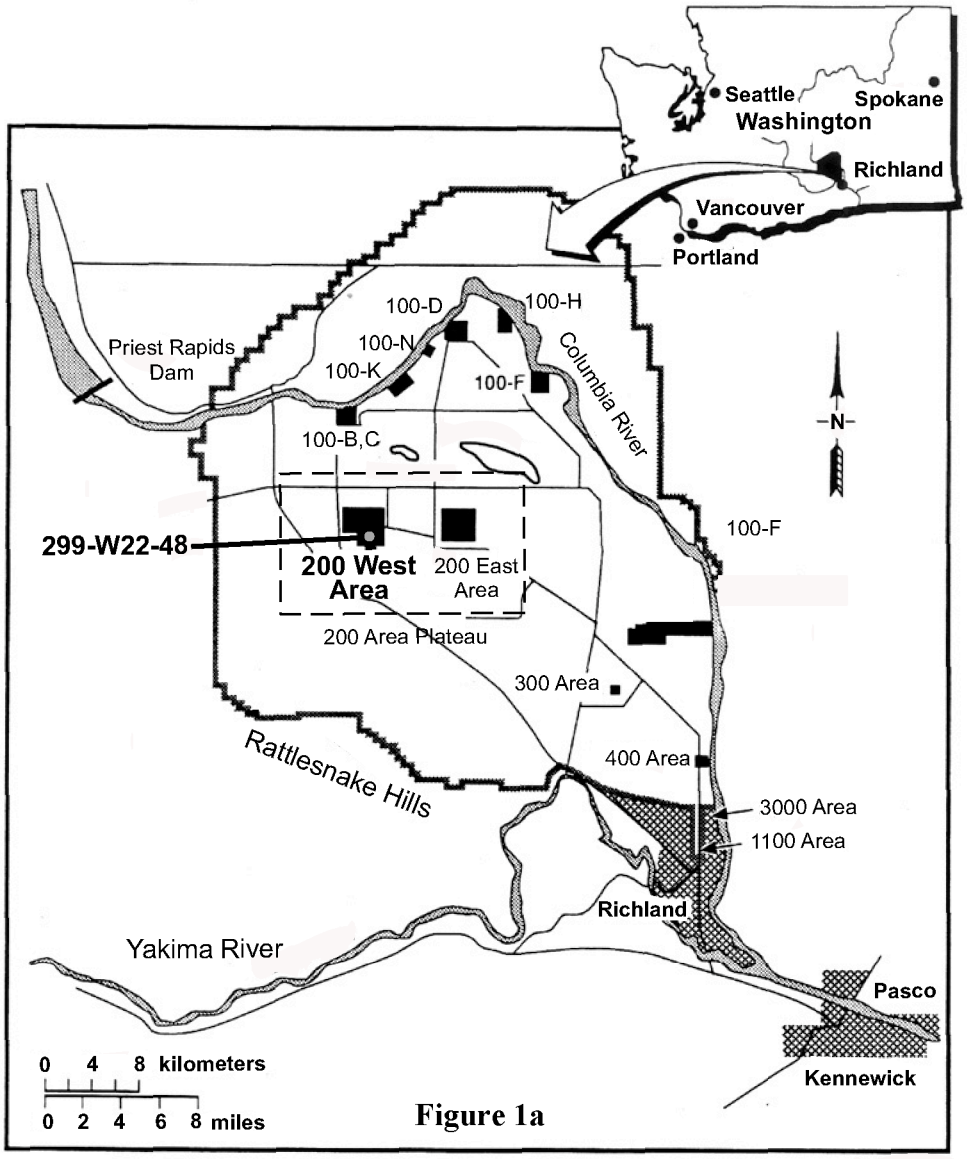

Figure 1a

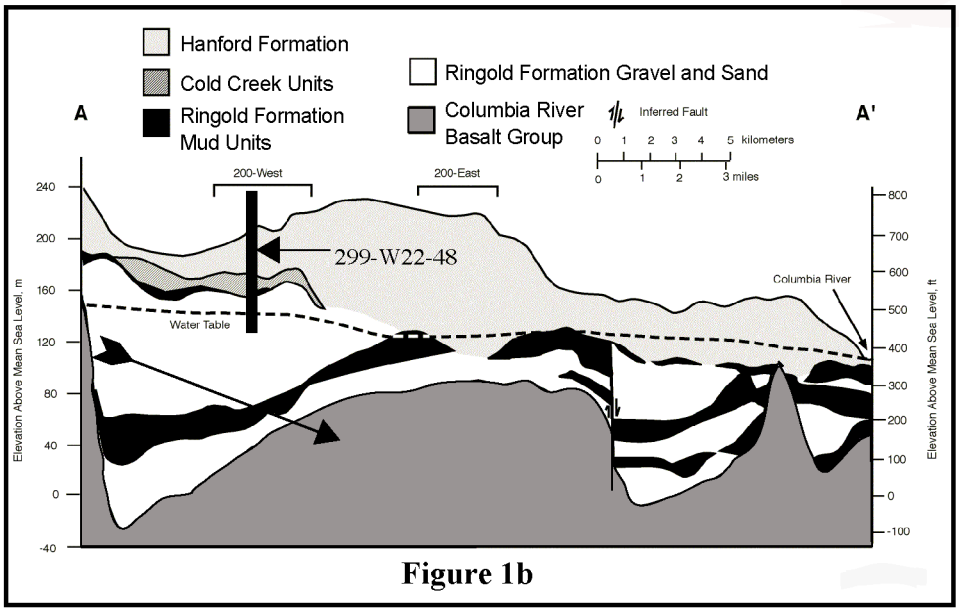

Figure 1b

Figure 1. (a) Hanford Site map showing location of 200 Area plateau and the 299-W22-48 bore hole and other pertinent locations. (b) Schematic cross–section depicting the predominant direction of groundwater flow.

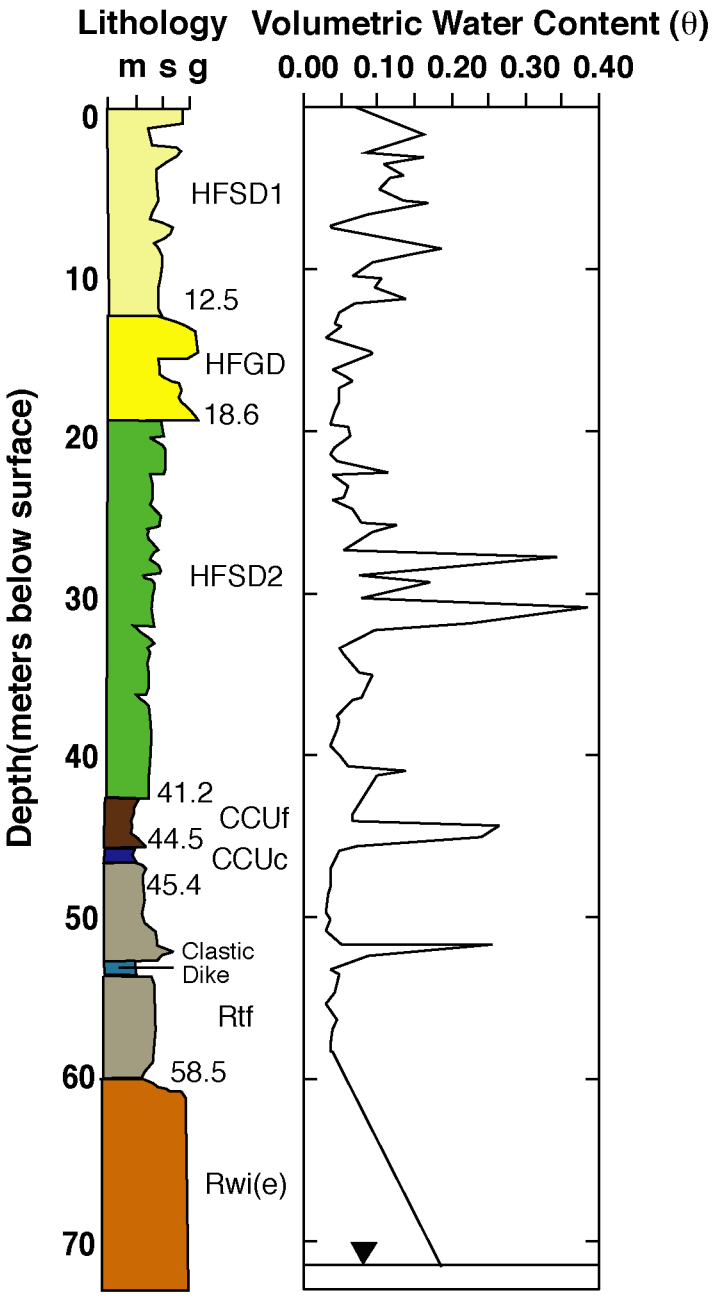

Figure 2. Lithology and Volumetric Water Content for the 299-W22-48 borehole. HFGD: Hanford Formation, gravel-dominated facies; HFSD: Hanford Formation, sand-dominated facies; CCUf(lam-msv): Cold Creek unit, silt and fine-grained sand; CCUc-f(calc): Cold Creek unit, calcic paleosol; Rtf: Ringold Formation, upper fines; Rwi: Ringold Formation, sandy gravel. (Data from Serne et al. [2002b] and US DOE [2002]).

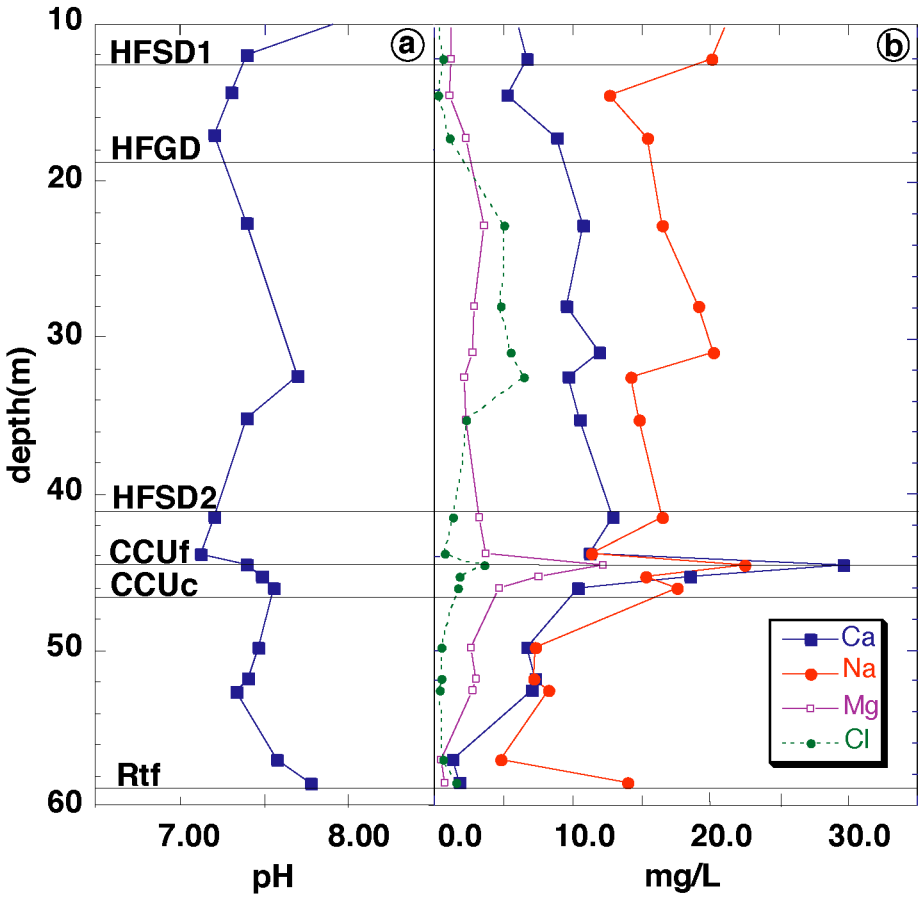

Figure 3. Background geochemical data for 1:1 sediment to deionized water extrtacts. (a) pH data for 1:1 sediment to deionized water extracts. (b) Chemical data for water extracts (ICP measurements from *Serne et al.*, [2002a]).

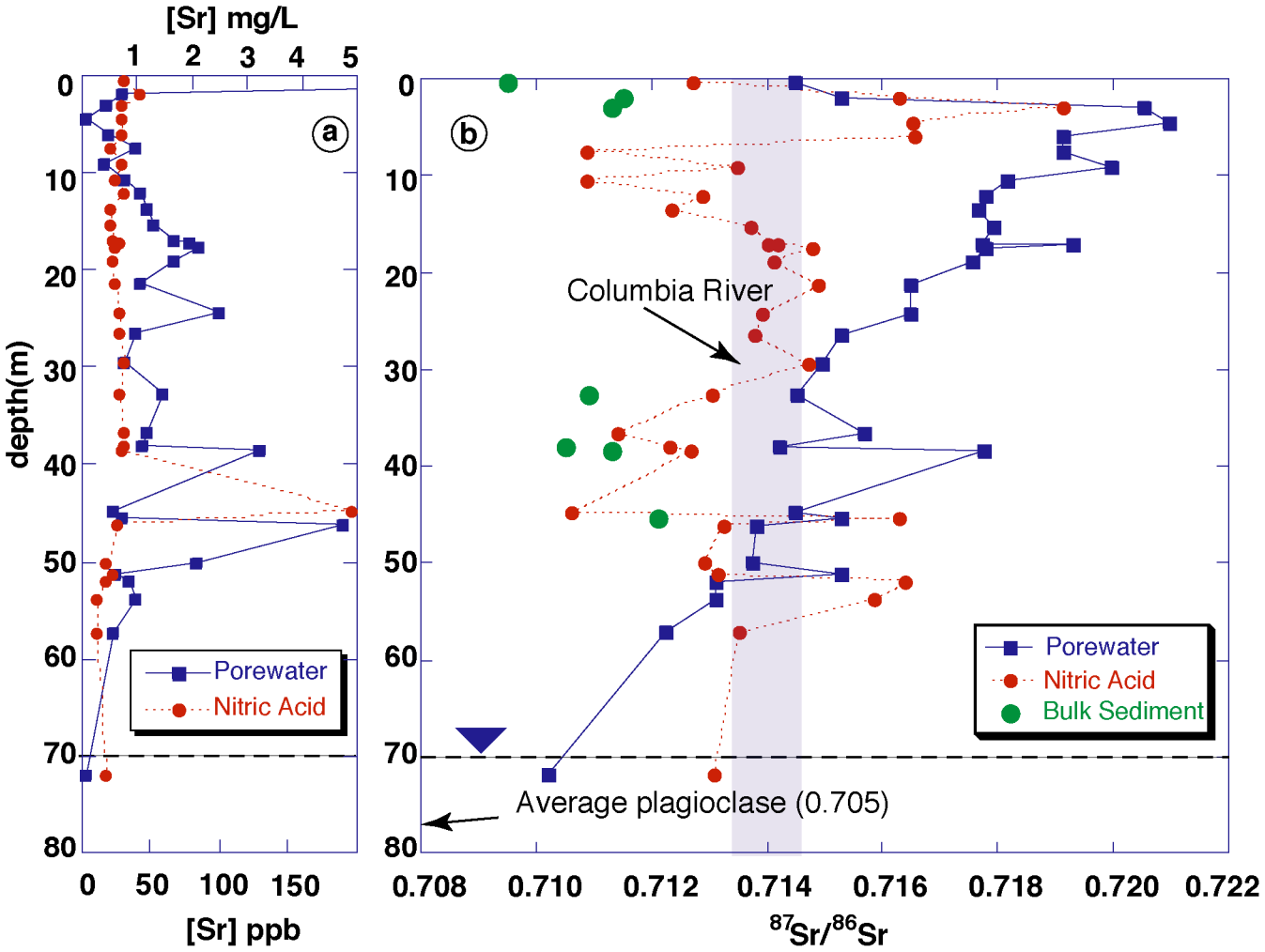

Figure 4. (a) Theoretical pore water Sr concentrations (mg/L) and nitric acid leaches (ppm). (b) $^{87}Sr/^{86}Sr$ profiles for pore waters, nitric acid leaches and bulk sediment. Columbia river values (0.7137-0.7144) and the approximate location of the unconfined aquifer are shown for reference.

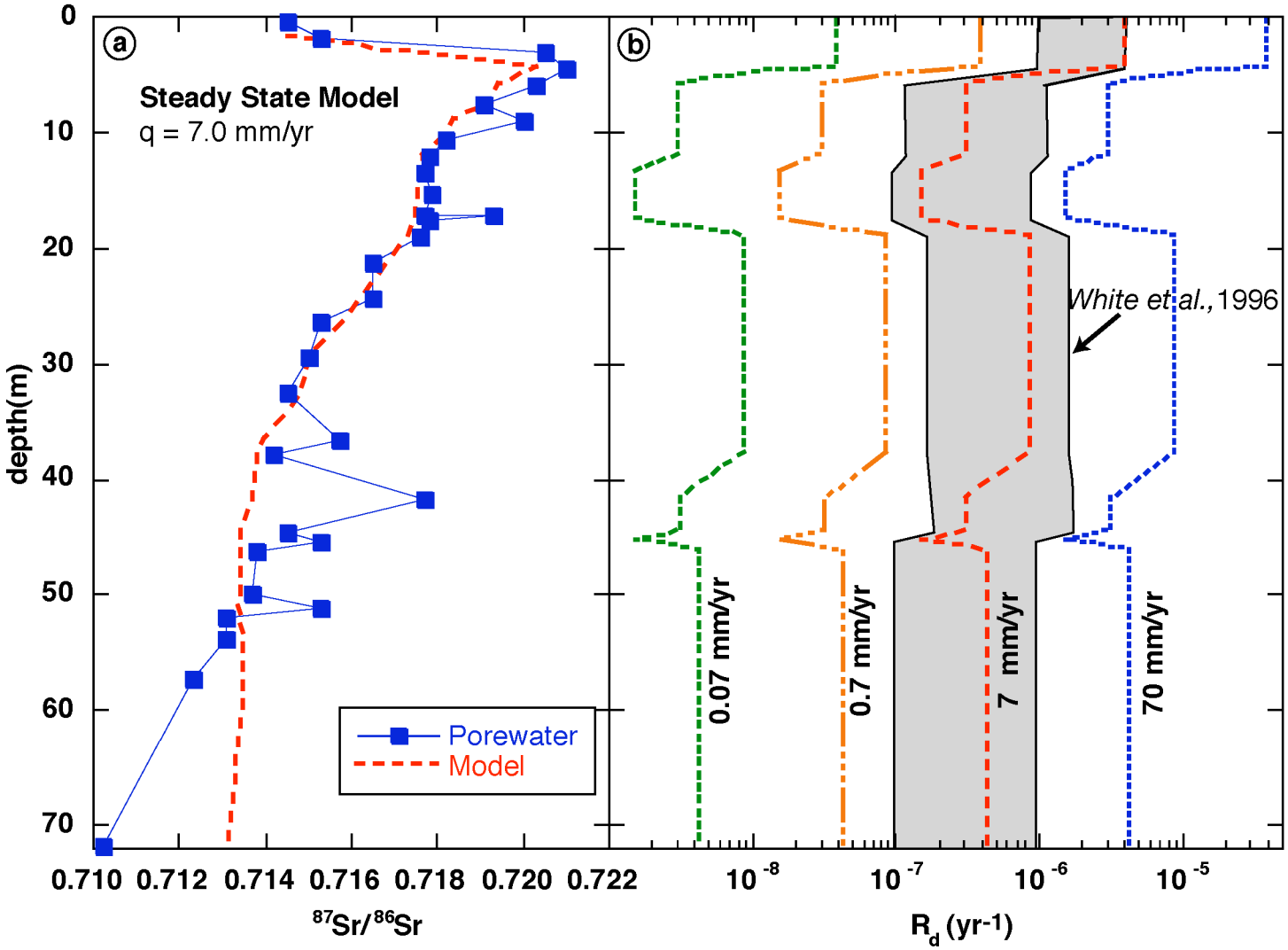

Figure 5. Steady State Model best-fit trajectory and R_d/v profile. (a) Best-fit trajectory corresponding to a dissolving solid $^{87}Sr/^{86}Sr$ ratio (r_d) of the nitric acid leach value and infiltration flux of 7 mm/yr. (b) Weathering rates required to fit the data for various infiltration rates. The estimated weathering rates are shown for reference. An order of magnitude change in the infiltration flux mandates a comparable change in the infiltration rate in order to fit the pore water data.

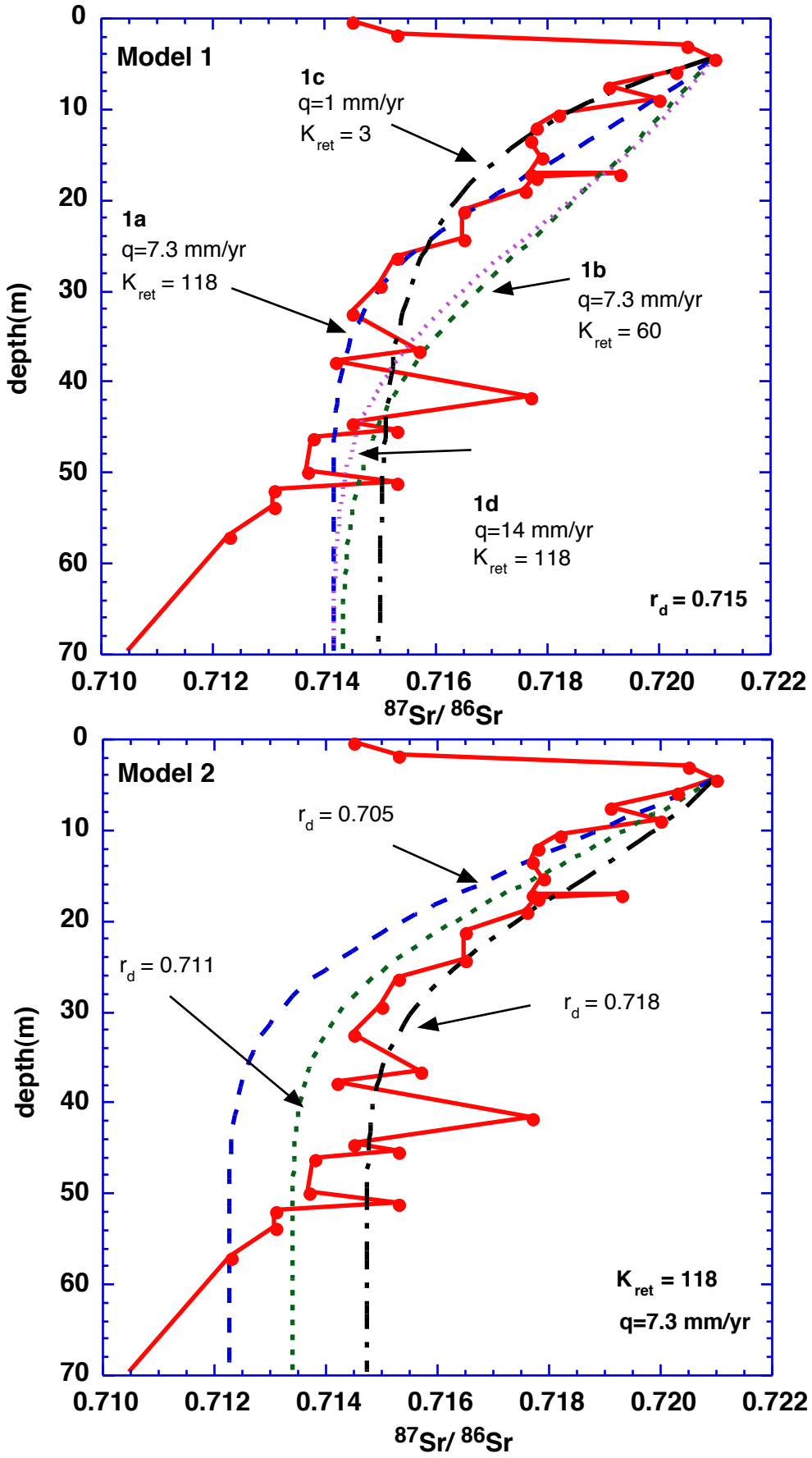

Figure 7: Non-Steady State Model, q = 0.09 and = 7m for all cases. (a) The effect of changes in the infiltration flux and retardation factor, (K_{ret}). (b) Model trajectories showing the effect of changes in the value of r_d.